**A peer-reviewed version of this preprint was published in PeerJ on 12 June 2018.**



Choi JI, Lee HK, Kim HS, Park SY, Lee TY, Yoon K, Lee JI. 2018. Odor-dependent temporal dynamics in *Caenorhabitis elegans* adaptation and aversive learning behavior. PeerJ 6:e4956
https://doi.org/10.7717/peerj.4956

# Odor-dependent temporal dynamics in *C. elegans* odor memory

**Jae Im Choi** [1] , **Hee Kyung Lee** [1] , **Hae Su Kim** [1] , **So Young Park** [1] , **Kyoung-hye Yoon** Corresp., [1] , **Jin I Lee** Corresp. [1]

[1] Division Of Biological Science and Technology, Yonsei University, Wonju, Gangwondo, South Korea

Corresponding Authors: Kyoung-hye Yoon, Jin I Lee
Email address: kyounghyeyoon@yonsei.ac.kr, jinillee@yonsei.ac.kr

Animals sense an enormous number of cues in their environments, and, over time, can form memories and associations to some of these. The nervous system remarkably maintains the specificity of memory to each of the cues. Here we asked whether the nematode *Caenorhabditis elegans* adjusts the temporal dynamics of odor memory formation depending on the specific odor sensed. *C. elegans* senses a multitude of odors, and memory formation to some of these odors requires activity of the cGMP-dependent protein kinase EGL-4 in the AWC sensory neuron. We identified a panel of 17 attractive odors, some of which have not been tested before, and determined that the majority of these odors require the AWC primary sensory neuron for sensation. We then devised a novel assay to assess odor behavior over time for a single population of animals. We used this assay to evaluate the temporal dynamics of memory formation to 13 odors and find that memory formation occurs early in some odors and later in others. We then examined EGL-4 localization in early-trending and late-trending odors over time and found that the timing of memory formation correlated with the timing of nuclear accumulation of EGL-4 in the AWC neuron. We demonstrate that odor memory formation in *C. elegans* can be used as a model to study the timing of memory formation to different sensory cues.

# Title: Odor-dependent temporal dynamics in *Caenorhabitis elegans* odor memory

**Authors:** Jae Im Choi**, Hee Kyung Lee**, Hae Su Kim**, So Young Park**, Kyoung-hye Yoon*, Jin I. Lee*

**Affiliation:** Division of Biological Science and Technology
Yonsei University
1 Yonseidae-gil
Wonju, Gangwondo
South Korea 26493

**Correspondence should be addressed to:**

Jin I. Lee (jinillee@yonsei.ac.kr)

Kyoung-hye Yoon (kyounghyeyoon@yonsei.ac.kr)

* Co-corresponding authors

** Co-first authors


## ABSTRACT

Animals sense an enormous number of cues in their environments, and, over time, can form memories and associations to some of these. The nervous system remarkably maintains the specificity of memory to each of the cues. Here we asked whether the nematode *Caenorhabditis elegans* adjusts the temporal dynamics of odor memory formation depending on the specific odor sensed. *C. elegans* senses a multitude of odors, and memory formation to some of these odors requires activity of the cGMP-dependent protein kinase EGL-4 in the AWC sensory neuron. We identified a panel of 17 attractive odors, some of which have not been tested before, and determined that the majority of these odors require the AWC primary sensory neuron for sensation. We then devised a novel assay to assess odor behavior over time for a single population of animals. We used this assay to evaluate the temporal dynamics of memory formation to 13 odors and find that memory formation occurs early in some odors and later in others. We then examined EGL-4 localization in early-trending and late-trending odors over time and found that the timing of memory formation correlated with the timing of nuclear accumulation of EGL-4 in the AWC neuron. We demonstrate that odor memory formation in *C. elegans* can be used as a model to study the timing of memory formation to different sensory cues.


## INTRODUCTION

The ability to form memories to odors is inherent to most animals. In particular, the formation of memories to biologically pertinent odors can be important for survival and reproduction. For instance, mother sheep form specific odor memories of their own lambs rather than other stranger lambs within hours of birth (Broad et al. 2002). This specific odor memory formation will be important for the mother sheep to establish bonding behaviors with her young (Levy et al. 2004).

The formation of a memory involves a step-by-step process defined by molecular and cellular activities within a determined circuitry. After a cue from the environment is recognized, the first stop along the path of the memory trace is a short-term memory (STM). In the sea snail *Aplysia*, short-term or intermediate-term memory in response to touch requires cell signaling events in the sensory neurons themselves (Ghirardi et al. 1995; Hawkins et al. 2006; Klein et al. 1982; Montarolo et al. 1986). Upon a strong and persistent cue, a robust and stable long-term memory (LTM) can form in response to changes in gene transcription and protein translation in *Aplysia* (Castellucci et al. 1970; Castellucci et al. 1989; Sutton et al. 2001). These changes require the kinase PKA to translocate from the cytoplasm to the nucleus to phosphorylate nuclear substrates and activate gene expression (Bacskai et al. 1993). The transition to long-term memory can be blocked and enhanced by a number of factors. For instance increased tyrosine kinase activity can reduce the cue threshold for long-term memory and enhance the LTM response, implicating that growth factors may facilitate LTM formation (Purcell et al. 2003). In addition, the phosphatase calcineurin can block the induction of LTM by counteracting kinase activity (Mansuy et al. 1998).

The nematode *Caenorhabditis elegans* is attracted to dozens or more odors and forms a memory in response to persistent odor stimulation in the absence of food (Bargmann et al. 1993; Colbert & Bargmann 1995; Ward 1973). A short 30 minute exposure to the odor benzaldehyde attenuates the attraction transiently. However, an 80 minute exposure eliminates the attraction for benzaldehyde for a prolonged period (Colbert & Bargmann 1995; Lee et al. 2010). Short-term memory to benzaldehyde requires kinase activity in the cytoplasm by the *C. elegans* PKG homolog EGL-4, whereas long-term odor memory requires EGL-4 to translocate to the nucleus and phosphorylate nuclear targets (Juang et al. 2013; L'Etoile et al. 2002; Lee et al. 2010; O'Halloran et al. 2009), similar to PKA nuclear translocation in *Aplysia*.

Although benzaldehyde odor memory has been thoroughly investigated, it is unknown whether strong memories to certain odors can form faster than to other odors. In this study we sought to investigate the temporal dynamics of memory formation to a large panel of odors by designing a new odor behavior assay called the real-time odor behavior assay. Using this novel assay, we found the timing of memory formation was specific for each odor, and temporal dynamics were correlated to the localization of EGL-4 in the AWC neuron.

## MATERIALS AND METHODS

*Nematode culture and strains*. Worms were grown and maintained at 20°C on Nematode Growth Medium (NGM) plates seeded with E. coli OP50 as described previously (Brenner 1974). Strains used for this study, N2, *ceh-36*, *odr-7, pyIs500* ((p)*odr-3*::GFP::*egl-4*), were obtained from the *Caenorhabditis* Genetic Center (University of Minnesota, USA).

*Behavior assays.* Standard odor chemotaxis assays were carried out using previously established protocols with a few changes (Bargmann et al. 1993). The following odors were used: benzaldehyde, butanone, isoamyl alcohol (Sigma-Aldrich, USA); isobutyric acid, 2-isobutyl thiazole, dimethylthiazole, 2,4,5-trimethylthiazole, 2-methylpyrazine, 2-heptanone, 4-chlorobenzyl mercaptan, butyric acid, 1-pentanol, benzyl mercaptan, 2-cycolhexylethanol, benzyl proprionate (Alfa Aesar, South Korea); 1-methylpyrrole, 2-ethoxythiazole (TCI, Japan); diacetyl (Acros Organics, Belgium). All odors were diluted from original stock to a 1:100 dilution with ethanol except for benzaldehyde (1:200) and 2,4,5-trimethylthiazole (1:1000). A total of 4 µl of diluted odor or ethanol was placed on the assay plate as attractant and counterattractant, respectively. 2 µl of $NaN_3$ was placed with the attractant and counterattractant. Briefly, adult worms were washed in S-basal buffer (5.85 g NaCl, 1 g $K_2HPO_4$, 6 g $KH_2PO_4$) 3 times, placed on the assay plate, and allowed to move freely for at least one hour before counting.

Standard odor memory behavior assays were carried out similar to previous published protocols (Colbert & Bargmann 1995). Before assaying behavior, worms were washed in S-basal buffer 3 times, and placed in 1 ml of benzaldehyde or 2,4,5-TMT diluted at 1:10,000 in S-basal buffer for 0-120 minutes at 10 minute or 20 minute intervals. After odor exposure, worms were washed 3 times in S-basal and behavior was assayed.

*Real-time odor behavior assay.* Media for the assay plate is as follows: 1.6% Difco Granulated Agar (BD, USA) was dissolved in water by heating, and 1mM of $CaCl_2$, 1mM of $MgSO_4$ and 5 mM

of $KPO_4$ buffer (108.3 g KH2PO4, 35.6 g K2HPO4, H2O to 1 liter) was mixed with the agar. Media was dispensed into 12.5 cm X 12.5 cm X 2 cm square plastic culture plates (SPL Bioscience, S. Korea), and allowed to harden for at least 3 hours. Odors were diluted with ethanol to the following concentrations: benzaldehyde (1:100), butanone (1:100), diacetyl (1:100), isoamyl alcohol (1:1000), 2-heptanone (1:1000), 2,4,5-TMT (1:500), 4-chlorobenzyl mercaptan (1:500), 2-ethoxythiazole (1:300), 2-cyclohexylethanol (1:5000), 1-methylpyrrole (1:500), 1-pentanol (1:10000), 2-isobutylthiazole (1:100), 2-methylpyrazine (1:10). Diluted attractant odors were placed in the middle of the "A" section of the assay plate (Figure 1), and a dab of OP50 strain *E. coli* bacteria from a standard nematode growth media plate with a platinum worm picker was placed in the middle of the "F" section of the assay plate as a counterattractant, no larger than 3 mm diameter. The counterattractant itself is a very weak attractant (Figure 1B, control), and overall aids this assay in resolving the attenuation of odor attraction after memory has formed. Washed worms are then placed in the middle of the plate, and dried by wicking the buffer using an unscented tissue. The plates were tapped somewhat vigorously which aids in worm movement away from the center of the plate. Worms were counted in each section A, B, E, and F every ten minutes for 120 minutes and attraction index was calculated. 50% total behavior change was calculated as (30 min AI – 120 min AI)/2.

*Quantification of GFP::EGL-4 localization*. Subcellular localization of GFP::EGL-4 in *py*Is500 ((p)*odr-3*::GFP::EGL-4; (p)*odr-1*::RFP) integrated strain worms during odor memory formation was performed as previously published (Lee et al. 2010). Briefly, *py*Is500 animals were exposed to odor dilutions of either benzaldehyde (1:10000), 2-ethoxythiazole (1:10000), 1-methylpyrrole

(1:10000), 4-chlorobenzyl mercaptan (1:5000), or 2,4,5-TMT (1:10000) in S-basal for 0-120 minutes at 20 minute intervals. After odor exposure, worms were placed on slides containing a 2% agar dried pad with 1 µl of 1M $NaN_3$ added to anesthetize the animals and observed under a fluorescent microscope. At least 20 animals were counted per sample, and EGL-4 localization was determined as either cytoplasmic or nuclear in the AWC neuron for each animal. After the data was plotted, a polynomial regression equation was determined (Microsoft Excel) for each odor as follows: benzaldehyde (y = 0.0308x4 - 1.1348x3 + 10.026x2 - 17.514x + 16.786), 2-ethoxythiazole (y = -0.1198x4 + 1.0243x3 - 0.599x2 + 4.9802x + 5.5179), 1-methylpyrrole (y = -0.2053x4 + 2.3015x3 - 5.4917x2 + 4.5729x + 8.4286), 4-chlorobenzyl mercaptan (y = -0.1454x4 + 1.8802x3 - 6.4253x2 + 11.766x + 1.0536), 2,4,5-TMT (y = 0.1437x4 - 2.599x3 + 15.825x2 - 27.302x + 22.06). Equations were used to calculate the approximate time at which 50% of animals display nuclear EGL-4.

## RESULTS

### Attraction to novel odors mediated by the AWC or the AWA primary sensory neurons

*C. elegans* is attracted to dozens of odors (Bargmann et al. 1993), and several forms of memory to a few of these odors have been demonstrated (Colbert & Bargmann 1995; Kauffman et al. 2010; L'Etoile et al. 2002; Torayama et al. 2007). To test the olfactory memory to a larger panel of odors, we screened through a large set of over 150 odor chemicals and identified dozens of attractive odors. From this smaller group, we tested attraction to a subset

of 18 highly attractive odors in wild-type and olfactory sensory neuron mutants in a standard chemotaxis assay (Bargmann et al. 1993).

Odor attraction in *C. elegans* is mediated by two pairs of olfactory sensory neurons, the AWC neurons and the AWA neurons. Mutants of the *ceh-36* gene which encodes an *Otx* homeodomain transcription factor do not develop AWC olfactory sensory neurons (Lanjuin et al. 2003), whereas mutants of the *odr-7* gene which encodes an AWA-specific nuclear hormone receptor lack the AWA sensory neurons (Sengupta et al. 1994). Thus, AWC-sensed odors such as benzaldehyde or butanone are unable to be sensed in *ceh-36* mutants, and, conversely, AWA-sensed odors such as diacetyl are no longer sensed in *odr-7* mutants. As predicted, we show that diacetyl attraction is lost in the AWA- *odr-7* mutants and maintained in *ceh-36* mutants (Table 1). On the contrary, benzaldehyde attraction disappears in the AWC- *ceh-36* mutants but is normal in AWA- *odr-7* mutants. Finally, 2,4,5-trimethylthiazole which is sensed by both AWA and AWC neurons remains attractive in both AWC- and AWA- mutants. When we tested the other odors, we found that attraction to most of the odors required the AWC sensory neurons, with only butyric acid and isobutyric acid sensed by the AWA neuron (Table 1). Benzyl proprionate attraction was effectively lost in both AWC- and AWA- mutants. Hence, we have identified many novel attractive AWC-sensed odors.

**A novel assay to track real-time odor behavior**

Short-term and long-term olfactory memory has been studied for the AWC-sensed odor benzaldehyde (Colbert & Bargmann 1995; L'Etoile et al. 2002; Lee et al. 2010). However, the

temporal dynamics of memory formation to other odors have not been tested thoroughly. Thus, we sought to characterize the change in odor attraction over time to a multitude of AWC-sensed odors. The standard odor treatment and chemotaxis assay protocol to measure *C. elegans* odor memory is a robust assay that has led to the discovery of odor memory mutants and revealed molecular pathways involved in memory formation (Bargmann et al. 1993; Colbert & Bargmann 1995; L'Etoile et al. 2002; Lin et al. 2010; O'Halloran et al. 2009). However, for a thorough temporal characterization of memory behavior for multiple odors, the standard assay would require a separate behavior assay for each time point for each odor, necessitating an inordinately large amount of worms and resources for such a study.

Due to the limitations of the standard odor memory behavior assay, we designed a new odor behavior assay we call the "real-time odor behavior assay". This method is based on a previously designed odor behavior assay (Remy & Hobert 2005), in which a population of worms is placed on the center of a larger 12.5 cm X 12.5 cm square plate rather than the 9 cm diameter circular plate used in the standard assay (Fig 1A). The plate is divided into 6 even columns labeled A-F, with a dilution of odor placed in the center of one of the side columns (column A). On the opposite side column (column F), a small spot of OP50 strain *E. coli* bacteria, a common laboratory source of food for *C. elegans*, is placed towards the middle and used as a counterattactant to the odor.

Worms can freely move throughout the whole plate for the entire 120 minute assay. We calculate the "attraction index" to the odor as AI = [[2(# of worms in A) + (# of worms in B)] – [(# of worms in E) + 2 (# of worms in F)]] / 2(# of worms in A+B+E+F), and the attraction index is counted every 10 minutes. Animals in the middle columns C and D where the worms originated

from are not counted. Thus, the maximum AI is 1.0 and the minimum AI is -1.0. In contrast to the control assay in which only the diluent ethanol without odor is placed in column A, worms exposed to a dilution of benzaldehyde in the real-time assay move towards the odor for the first 30 minutes, with many animals reaching the attractive odor by 40 minutes (Figure 1B). After another 30 minutes we observed a slight decline in attraction, and finally at 90 minutes we observed a steep decline in attraction that maintained until the end of the assay.

**Short-term and long-term memory in the real-time odor behavior assay**

In the standard behavior assay, continuous odor exposure in the absence of food for about 30 minutes results in a partial and transient attenuation of attraction to benzaldehyde ((Colbert & Bargmann 1995; L'Etoile et al. 2002); Figure 2A). This short-term memory requires activity of the cGMP-dependent protein kinase EGL-4 (L'Etoile et al. 2002) and the cyclic nucleotide-gated channel subunit CNG-3 (O'Halloran et al. 2017). *cng-3* mutants do not display short-term odor memory, but display normal long-term memory to benzaldehyde ((O'Halloran et al. 2017); Fig 2A), which occurs after over 80 minutes of continuous benzaldehyde exposure. On the other hand, the dominant mutation *adp-1* displays no odor memory even after a 120 minute odor exposure ((Colbert & Bargmann 1995); Fig 2A).

In contrast to the standard assay technique in which odor exposure precedes the behavior assay, animals are concurrently exposed to benzaldehyde as the real-time assay proceeds. In the beginning of the assay, most of the freely moving worms can reach the odor at the far end of the plate within 30 minutes. Thus, to compare the two assay techniques, we

consider the 30 minute time point to be the "beginning" of the memory assay similar to the 0 minute time point in the standard assay. After the 30 minute time point wild-type *C. elegans* begins to display a decreased attraction for the next 40 minutes similar to that observed during short-term memory in the standard assay (Fig 2A, 2B). In *cng-3* mutants, however, this early change in behavior appears to be absent (Fig 2A, 2B).

A major difference between the two assay techniques is that each time point in the standard assay is an independent population of animals, whereas a single population is being tracked in the real-time assay. Thus, each data point is dependent on the previous data point in the real-time assay. This can lead to a decrease in resolution in data over time especially at close time points. To confirm that the real-time assay can indeed measure odor memory states in *C. elegans* similar to the standard assay, we compared attraction at the 0 and 40 minute time points in the standard assay to the 30 and 70 minute time points in the real-time assay. In both the standard and real-time assays, wild-type N2 animals display a significant decrease in attraction after 40 minutes (Fig 2C). Interestingly, this decrease was absent in short-term memory-defective *cng-3* mutants for both the standard and real-time assays (Fig 2C). However, a significant drop in attraction was observed after 80 minutes in both N2 and *cng-3* mutants, showing that long-term memory is intact in *cng-3* mutants (Fig 2B). Finally, no memory to benzaldehyde develops in *adp-1* mutants in either the standard assay or the new assay (Fig 2A, 2B). Thus, both short-term and long-term memory can be resolved in the real-time behavior assay.

**Timing of odor memory formation varies by odor**

Since we demonstrated that our assay can accurately assess the timing of benzaldehyde memory, we conducted a comprehensive temporal analysis of memory to a palette of 12 other odors, 9 of which have never been tested for memory. These include alcohols, ketones, thiols, thiazoles, aromatics, and pyrazines. 30 minutes into the assay when we start the analysis, we observe differences in attraction to each odor ranging from 0.91 AI (2,4,5-trimethylthiazole) to 0.50 AI (2-heptanone). However, over time, the total decrease in attraction to all of the odors is similar over the entire assay (average AI decrease=-0.475±0.025) with one exception, the odor cyclohexylethanol, which displays only a modest attenuation (AI decrease=-0.19).

Among the panel of 13 odors tested, 12 of these odors are sensed by the AWC neuron. One can observe a distinct pattern of change in worm behavior towards these twelve odors over time. For AWC-sensed odors, behavior change generally occurs relatively slowly at the beginning of the assay then proceeds more quickly towards the end (Figure 3). The exception to this is the odor diacetyl, which is the only odor here not sensed by the AWC neuron. Behavior change towards diacetyl appears to arise early and fairly consistently during the entire assay (Figure 3).

Although overall memory formation patterns over the 120 minute assay is similar for most of the odors tested, the timing of memory formation varies depending on the odor. For instance, benzaldehyde attraction decreases overall from 0.79 AI to 0.27 from 30 to 120 minutes, and 50% of this behavior change occurs within the 90 minute mark (Figure 3; Table 2). This early trend was similar to that of 2-ethoxythiazole attraction (90 min) and 1-methylpyrrole

attraction (80 minutes). On the other hand, late trends of behavior change were observed in 2,4,5-trimethylthiazole (2,4,5-TMT) attraction (100 minutes) and 4-chlorobenzyl mercaptan (4-CB) attraction (110 minutes) (Figure 3, Table 2). To confirm whether the late change in behavior was actually a result of odor memory, we tested the attraction of *adp-1* mutants to 4-chlorobenzyl mercaptan and 2,4,5-TMT attraction in the real-time assay (Figure S1). Wild-type animals showed large decreases in attraction over the whole assay for both 4-CB (change in AI=-0.478) and 2,4,5-TMT (change in AI=-0.349). However, the change in behavior over time was minimal in *adp-1* mutants for both 4-CB attraction (change in AI=-0.226) and 2,4,5-TMT attraction (change in AI=-0.009). Thus, the late trend in decreased odor attraction for the two odors is likely due to late odor memory formation. We also confirmed that the early trend in benzaldehyde memory and the late trend in 2,4,5-TMT memory can be observed using either the real-time assay or the standard assay (Figure S2). Thus, temporal dynamics of memory formation varies depending on the specific odor.

**Timing of odor memory formation correlates with the timing of EGL-4 nuclear localization**

With the exception of diacetyl which is sensed only by the AWA neuron, all the odors we tested in the real-time assay are sensed by the AWC neuron (Table 1). Odor memory to AWC-sensed odors requires EGL-4 activity: cytoplasmic EGL-4 activity directs short-term memory whereas long-term memory requires EGL-4 to translocate to the nucleus and phosphorylate nuclear targets (Juang et al. 2013; L'Etoile et al. 2002). We wondered whether the changes in odor attraction we observe over time in the real-time assay were correlated to the sub-cellular

localization of a functional GFP-tagged EGL-4 in the AWC neuron. We exposed worms to the early-trending odors (benzaldehyde, 2-ethoxythiazole, 1-methylpyrrole) and the late-trending odors (2,4,5-trimethylthiazole, 4-chlorobenzyl mercaptan) and observed EGL-4 localization in the AWC neuron every 20 minutes for 2 hours. Whereas the odor butanone is sensed by one of the AWC neuron pair and EGL-4 nuclear translocation is induced in only one of the AWC neurons, all the odors tested here could induce EGL-4 translocation in both AWC neurons indicating that these odors are likely sensed by both AWC neurons. The maximal percent of animals with nuclear EGL-4 ranged from 60% to almost 80% for each odor (Figure 4). However, neither longer odor incubation nor varying odor concentration could increase maximal nuclear EGL-4 for benzaldehyde, 4-chlorobenzyl mercaptan or 2,4,5-trimethylthiazole (data not shown).

The temporal dynamic of EGL-4 nuclear localization in response to the early- and late-trending odors seems to vary depending on the odor. To analyze this in detail, we calculated a polynomial regression for the time curves for each odor (Figure 4), and then estimated the time at which 50% EGL-4 nuclear localization was reached for each odor (Table 2). We found that EGL-4 nuclear localization occurred much faster in the early trending odors (59.2 min, 69.7 min, 76.6 min for 2-ethoxythiazole, benzaldhehyde and 2-methylpyrrole, respectively), and occurred much later in the late-trending odors (88.4 min and 90.96 min for 4-CB and 2,4,5-TMT, respectively). Thus, we saw a correlation between the timing of EGL-4 nuclear translocation and the timing of odor memory formation. Taken together, we believe that the timing of odor memory formation for AWC-sensed odors may be regulated by EGL-4 sub-cellular localization.

## DISCUSSION

Establishing the real-time behavior assay was the key to comprehensively testing temporal dynamics of memory to multiple odors. This assay has several advantages to the standard assay that has been valuable in understanding odor behavior in *C. elegans*. Firstly, tracking a single population over time rather than independent populations at each time point has benefits. For instance, we can observe actual changes in the behavior of animals over time, decrease experimental variability between populations, and save time and resources tracking one population rather than 13 populations over the 120 minute assay. Finally, the real-time assay is a better simulation of odor behaviors in natural habitats than the standard assay. Our group previously showed that production of the odor diacetyl in rotting fruit attracts *C. elegans* (Choi et al. 2016). The new assay allows worms to freely move on a large field and alter their behavior towards the odor over time more similar to natural habitats.

Although tracking a single population over time has advantages, this results in each data point being dependent on the previous data point. This leads to a decrease in resolution in data over time that is not a problem in the standard assay. Due to this concern we tested whether different behavioral states in *C. elegans* mutants can be resolved in the real-time assay. We found that short-term odor memory defects were observed in *cng-3* mutants in the real-time assay as has been observed in the standard assay (O'Halloran et al. 2017). Still, the standard assay has stronger behavior resolving power than our new assay particularly in identifying behavior mutants. The real-time assay cannot replace the standard behavior assay but can supplement it with an ability to observe temporal dynamics on a large scale and also simulate natural odor behaviors.

Using the real-time assay we were able to identify odors in which memory forms early in *C. elegans* such as 1-methylpyrrole, and odors in which memory forms late such as 4-chlorobenzyl mercaptan. Since formation of long-term memory to AWC-sensed odors requires EGL-4 nuclear translocation, we exposed worms to early-trending and late-trending odors and observed EGL-4 localization over time. We found a correlation between the timing of memory formation and nuclear accumulation. How then do specific odors regulate the timing of EGL-4 nuclear translocation? Long-term odor memory in the AWC neuron is dependent on the coincident detection of food deprivation that is mediated by insulin signaling from the AIA neuron (Cho et al. 2016). Insulin signals from the AIA activate the PI3 kinase AGE-1 in the AWC neuron to promote EGL-4 nuclear accumulation. However, food deprivation is stable from odor to odor in our experiments, thus AIA neuron-dependent insulin signals likely cannot account for the differences observed in odor-dependent EGL-4 nuclear translocation. Within the AWC neuron, the G-protein ODR-3 and cGMP levels have both been shown to regulate nuclear EGL-4 localization (O'Halloran et al. 2009; O'Halloran et al. 2012). Specific odors, and possibly specific G-protein coupled olfactory receptors, may target ODR-3 and/or cGMP machinery which includes the guanylyl cyclases ODR-1 and DAF-11 and AWC-specific phosphodiesterases to regulate the timing of EGL-4 nuclear localization (Birnby et al. 2000; L'Etoile & Bargmann 2000; Roayaie et al. 1998). Further experiments that identify new olfactory receptors in the AWC neuron will elucidate the specific mechanisms.

One possible explanation of the differences in odor memory formation is that odor attraction and memory is concentration-dependent. For this reason, we tested several dilutions for most of the odors analyzed in the real-time behavior assay (data not shown), and finally

chose the optimal dilution for each odor in which behavior change was greatest over the entire experiment. In this way, we observed that the collective change in attraction over the whole assay was very similar for 12 of 13 odors tested. Despite overall similarities at the optimal concentrations, temporal patterns of behavior change were still varied among the odors.

We also tested memory formation to the AWA-sensed odor diacetyl and found that memory formed faster and more consistently than AWC-sensed odors. In addition, the odor 2,4,5-trimethylthiazole is sensed by both AWA and AWC neurons. Interestingly, we found that 2,4,5-TMT induced EGL-4 nuclear accumulation in the AWC neuron, and memory formation was correlated to late EGL-4 translocation. Further testing with AWA-sensed odors such as pyrazine (Bargmann et al. 1993) and butyric acid and isobutyric acid (Table 1) may reveal whether fundamentally different mechanisms of odor memory formation exist between the AWA and AWC neurons.

In this study, we investigated *C. elegans* response to many odors, including odors that have not been tested on *C. elegans* before, and identified the sensory neuron responsible for each odor attraction. In addition, we tested the memory formation towards 13 of the odors over time. Such inherent behaviors towards the odors indicates that these odors may be ecologically relevant cues for *C. elegans* in nature. For instance, 2-isobutylthiazole is a major component of antelope pheromone (Burger et al. 1988), 2-methylpyrazine is the main volatile component of grape vinegar (Pinu et al. 2016), and butyric acid is produced by microbial fermentation (Pasteur 1861). Indeed, studies have shown ecologically relevant relationships between *C. elegans* and diacetyl (Choi et al. 2016), methyl 3-methyl-2-butenoate (Hsueh et al. 2017), and 2-heptanone (Zhang et al. 2016), and mammalian predator-prey relationships

between 2,4,5-TMT, a component of fox feces, and rodents (Vernet-Maury 1980). Finally, we found that memory does not form towards cyclohexylethanol. The ecological implications of a persistent attraction to this odor is unknown. Cyclohexylethanol derivatives were found in a plant root extract widely used in Chinese folk medicine (Huang et al. 2009), but relationships with nematodes need to be further investigated. We hope that this study can be a platform for more studies into natural odor behaviors.

## CONCLUSION

Dynamics of memory formation may vary depending on the cue that is learned. Since *C. elegans* can form memories to a multitude of odor cues, we devised a new behavioral assay to efficiently examine the temporal dynamics of odor memory formation to over a dozen odors. Using the real-time behavior assay, we found that worms form memories to certain odors faster than others. Finally, we investigated the cellular basis for this difference and found that rate of EGL-4 nuclear translocation for each odor was correlated to the rate of memory formation.

## ACKNOWLEDGEMENTS

We would like to thank the Caenorhabditis Genetic Center which is supported by the by NIH Office of Research Infrastructure Programs for strains, and the Korean Creative Foundation for the Undergraduate Research Program.

**FIGURE LEGENDS**

Figure 1. Real-time odor behavior assay. (A) Assay design. Worms are placed in the middle of a 15 cm square plate. Odor solution is placed on one side of the plate, and a weak counterattractant (*E. coli* strain OP50) is placed on the opposite side. (B) Benzaldehyde attraction in real-time odor behavior assay. Attraction to the odor benzaldehyde (blue) decreases over the 2 hour assay. Control diluent (100% ethanol) attraction is shown in red.

Figure 2. Short-term and long-term odor memory to the odor benzaldehyde in the real-time odor behavior assay. Attraction over time with N2 wild type, *cng-3* short-term odor memory defective mutants, and *adp-1* short-term and long-term odor memory mutants in the standard behavior assay (A) and the real-time odor behavior assay (B). (C) Short-term odor memory in the standard and real-time behavior assays. Comparison of the 0' and 40' minute time points in (A) with the 30' and 70' minute time points in (B) for N2 and *cng-3* mutants. Error bars indicate standard error. Statistical significance calculated by student's T-test. * indicates $p<0.05$, ** indicates $p<0.001$, NS indicates not significant.

Figure 3. Temporal dynamics of odor memory to 12 odors. Purple dotted line marks approximate place where 50% of total behavior change occurs for each odor. Error bars indicate standard error.

Figure 4. GFP::EGL-4 nuclear accumulation in early and late trending odors. Animals were exposed to odor for indicated time and cytoplasmic/nuclear GFP::EGL-4 localization was observed. Early-trending odors are on the left, and late-trending odors on the right. A polynomial regression was calculated and regression curves are indicated on each graph. See Methods for individual regression equations. Error bars indicate standard error.

Table 1. AWC and AWA primary sensory neurons primary sensory neurons mediate the attraction to 17 odors. Wild-type indicates N2 strain, AWC- indicates the ceh-36 mutant strain, AWA- indicates odr-7 mutant strain. Right column indicates the neuron(s) responsible for sensing each odor. Extra large dot = 0.6-1.0 attraction index (AI), large dot = 0.4-0.6 AI, medium dot = 0.2-0.4 AI, and small dot < 0.2 AI.

Table 2. Timing of behavior change correlates with timing of GFP::EGL-4 nuclear accumulation. Minutes to 50% animals with nuclear EGL-4 was calculated from the polynomial regression equation (see Methods) for each odor.

Figure S1. *adp-1* mutants do not display odor memory to 4-chlorobenzyl mercaptan and 2,4,5-trimethylthiazole. Attraction to 4-chlorobenzyl mercaptan (top) and 2,4,5-trimethylthiazole

(bottom) in the real-time behavior assay in wild-type N2 (blue) and *adp-1* mutant animals (orange). Error bars indicate standard error.

Figure S2. *C. elegans* displays late memory formation to 2,4,5-trimethylthiazole in the standard assay. Wild-type N2 animals show early memory formation to the odor benzaldehyde (dark blue), and late memory formation to 2,4,5-trimethylthiazole (red). Error bars indicate standard error.

**REFERENCES**

Bacskai BJ, Hochner B, Mahaut-Smith M, Adams SR, Kaang BK, Kandel ER, and Tsien RY. 1993. Spatially resolved dynamics of cAMP and protein kinase A subunits in Aplysia sensory neurons. *Science* 260:222-226.

Bargmann CI, Hartwieg E, and Horvitz HR. 1993. Odorant-selective genes and neurons mediate olfaction in C. elegans. *Cell* 74:515-527.

Birnby DA, Link EM, Vowels JJ, Tian H, Colacurcio PL, and Thomas JH. 2000. A transmembrane guanylyl cyclase (DAF-11) and Hsp90 (DAF-21) regulate a common set of chemosensory behaviors in caenorhabditis elegans. *Genetics* 155:85-104.

Brenner S. 1974. The genetics of Caenorhabditis elegans. *Genetics* 77:71-94.

Broad KD, Hinton MR, Keverne EB, and Kendrick KM. 2002. Involvement of the medial prefrontal cortex in mediating behavioural responses to odour cues rather than olfactory recognition memory. *Neuroscience* 114:715-729.

438 Burger BV, Pretorius PJ, Stander J, and Grierson GR. 1988. Mammalian pheromone studies, VII.
439 Identification of thiazole derivatives in the preorbital gland secretions of the grey duiker,
440 Sylvicapra grimmia, and the red duiker, Cephalophus natalensis. *Z Naturforsch C* 43:731-
441 736.
442 Castellucci V, Pinsker H, Kupfermann I, and Kandel ER. 1970. Neuronal mechanisms of
443 habituation and dishabituation of the gill-withdrawal reflex in Aplysia. *Science* 167:1745-
444 1748.
445 Castellucci VF, Blumenfeld H, Goelet P, and Kandel ER. 1989. Inhibitor of protein synthesis
446 blocks long-term behavioral sensitization in the isolated gill-withdrawal reflex of Aplysia.
447 *J Neurobiol* 20:1-9. 10.1002/neu.480200102
448 Cho CE, Brueggemann C, L'Etoile ND, and Bargmann CI. 2016. Parallel encoding of sensory
449 history and behavioral preference during Caenorhabditis elegans olfactory learning. *Elife*
450 5. 10.7554/eLife.14000
451 Choi JI, Yoon KH, Subbammal Kalichamy S, Yoon SS, and Il Lee J. 2016. A natural odor attraction
452 between lactic acid bacteria and the nematode Caenorhabditis elegans. *ISME J* 10:558-
453 567. 10.1038/ismej.2015.134
454 Colbert HA, and Bargmann CI. 1995. Odorant-specific adaptation pathways generate olfactory
455 plasticity in C. elegans. *Neuron* 14:803-812.
456 Ghirardi M, Montarolo PG, and Kandel ER. 1995. A novel intermediate stage in the transition
457 between short- and long-term facilitation in the sensory to motor neuron synapse of
458 aplysia. *Neuron* 14:413-420.

459 Hawkins RD, Kandel ER, and Bailey CH. 2006. Molecular mechanisms of memory storage in
460 Aplysia. *Biol Bull* 210:174-191. 10.2307/4134556
461 Hsueh YP, Gronquist MR, Schwarz EM, Nath RD, Lee CH, Gharib S, Schroeder FC, and Sternberg
462 PW. 2017. Nematophagous fungus Arthrobotrys oligospora mimics olfactory cues of sex
463 and food to lure its nematode prey. *Elife* 6. 10.7554/eLife.20023
464 Huang ZS, Pei YH, Shen YH, Lin S, Liu CM, Lu M, and Zhang WD. 2009. Cyclohexyl-ethanol
465 derivatives from the roots of Incarvillea mairei. *J Asian Nat Prod Res* 11:523-528.
466 10.1080/10286020902927872
467 Juang BT, Gu C, Starnes L, Palladino F, Goga A, Kennedy S, and L'Etoile ND. 2013. Endogenous
468 nuclear RNAi mediates behavioral adaptation to odor. *Cell* 154:1010-1022.
469 10.1016/j.cell.2013.08.006
470 Kauffman AL, Ashraf JM, Corces-Zimmerman MR, Landis JN, and Murphy CT. 2010. Insulin
471 signaling and dietary restriction differentially influence the decline of learning and
472 memory with age. *PLoS Biol* 8:e1000372. 10.1371/journal.pbio.1000372
473 Klein M, Camardo J, and Kandel ER. 1982. Serotonin modulates a specific potassium current in
474 the sensory neurons that show presynaptic facilitation in Aplysia. *Proc Natl Acad Sci U S*
475 *A* 79:5713-5717.
476 L'Etoile ND, and Bargmann CI. 2000. Olfaction and odor discrimination are mediated by the C.
477 elegans guanylyl cyclase ODR-1. *Neuron* 25:575-586.
478 L'Etoile ND, Coburn CM, Eastham J, Kistler A, Gallegos G, and Bargmann CI. 2002. The cyclic
479 GMP-dependent protein kinase EGL-4 regulates olfactory adaptation in C. elegans.
480 *Neuron* 36:1079-1089.

481 Lanjuin A, VanHoven MK, Bargmann CI, Thompson JK, and Sengupta P. 2003. Otx/otd
482 homeobox genes specify distinct sensory neuron identities in C. elegans. *Dev Cell* 5:621-
483 633.
484 Lee JI, O'Halloran DM, Eastham-Anderson J, Juang BT, Kaye JA, Scott Hamilton O, Lesch B, Goga
485 A, and L'Etoile ND. 2010. Nuclear entry of a cGMP-dependent kinase converts transient
486 into long-lasting olfactory adaptation. *Proc Natl Acad Sci U S A* 107:6016-6021.
487 10.1073/pnas.1000866107
488 Levy F, Keller M, and Poindron P. 2004. Olfactory regulation of maternal behavior in mammals.
489 *Horm Behav* 46:284-302. 10.1016/j.yhbeh.2004.02.005
490 Lin CH, Tomioka M, Pereira S, Sellings L, Iino Y, and van der Kooy D. 2010. Insulin signaling plays
491 a dual role in Caenorhabditis elegans memory acquisition and memory retrieval. *J*
492 *Neurosci* 30:8001-8011. 10.1523/JNEUROSCI.4636-09.2010
493 Mansuy IM, Mayford M, Jacob B, Kandel ER, and Bach ME. 1998. Restricted and regulated
494 overexpression reveals calcineurin as a key component in the transition from short-term
495 to long-term memory. *Cell* 92:39-49.
496 Montarolo PG, Goelet P, Castellucci VF, Morgan J, Kandel ER, and Schacher S. 1986. A critical
497 period for macromolecular synthesis in long-term heterosynaptic facilitation in Aplysia.
498 *Science* 234:1249-1254.
499 O'Halloran DM, Altshuler-Keylin S, Lee JI, and L'Etoile ND. 2009. Regulators of AWC-mediated
500 olfactory plasticity in Caenorhabditis elegans. *PLoS Genet* 5:e1000761.
501 10.1371/journal.pgen.1000761

O'Halloran DM, Altshuler-Keylin S, Zhang XD, He C, Morales-Phan C, Yu Y, Kaye JA, Brueggemann C, Chen TY, and L'Etoile ND. 2017. Contribution of the cyclic nucleotide gated channel subunit, CNG-3, to olfactory plasticity in Caenorhabditis elegans. *Sci Rep* 7:169. 10.1038/s41598-017-00126-7

O'Halloran DM, Hamilton OS, Lee JI, Gallegos M, and L'Etoile ND. 2012. Changes in cGMP levels affect the localization of EGL-4 in AWC in Caenorhabditis elegans. *PLoS One* 7:e31614. 10.1371/journal.pone.0031614

Pasteur L. 1861. On the viscous fermentation and the butyrous fermentation. *Bulletin de la Société Chimique de France* 11:30–31.

Pinu FR, de Carvalho-Silva S, Trovatti Uetanabaro AP, and Villas-Boas SG. 2016. Vinegar Metabolomics: An Explorative Study of Commercial Balsamic Vinegars Using Gas Chromatography-Mass Spectrometry. *Metabolites* 6. 10.3390/metabo6030022

Purcell AL, Sharma SK, Bagnall MW, Sutton MA, and Carew TJ. 2003. Activation of a tyrosine kinase-MAPK cascade enhances the induction of long-term synaptic facilitation and long-term memory in Aplysia. *Neuron* 37:473-484.

Remy JJ, and Hobert O. 2005. An interneuronal chemoreceptor required for olfactory imprinting in C. elegans. *Science* 309:787-790. 10.1126/science.1114209

Roayaie K, Crump JG, Sagasti A, and Bargmann CI. 1998. The G alpha protein ODR-3 mediates olfactory and nociceptive function and controls cilium morphogenesis in C. elegans olfactory neurons. *Neuron* 20:55-67.

Sengupta P, Colbert HA, and Bargmann CI. 1994. The C. elegans gene odr-7 encodes an olfactory-specific member of the nuclear receptor superfamily. *Cell* 79:971-980.

524 Sutton MA, Masters SE, Bagnall MW, and Carew TJ. 2001. Molecular mechanisms underlying a
525 unique intermediate phase of memory in aplysia. *Neuron* 31:143-154.
526 Torayama I, Ishihara T, and Katsura I. 2007. Caenorhabditis elegans integrates the signals of
527 butanone and food to enhance chemotaxis to butanone. *J Neurosci* 27:741-750.
528 10.1523/JNEUROSCI.4312-06.2007
529 Vernet-Maury E. 1980. Trimethyl-thiazoline in fox feces: A natural alarming substance for the
530 rat In: Van Der Starr H, editor. International Symposium on Olfaction and Taste: IRL
531 Press. p 407.
532 Ward S. 1973. Chemotaxis by the nematode Caenorhabditis elegans: identification of
533 attractants and analysis of the response by use of mutants. *Proc Natl Acad Sci U S A*
534 70:817-821.
535 Zhang C, Zhao N, Chen Y, Zhang D, Yan J, Zou W, Zhang K, and Huang X. 2016. The Signaling
536 Pathway of Caenorhabditis elegans Mediates Chemotaxis Response to the Attractant 2-
537 Heptanone in a Trojan Horse-like Pathogenesis. *J Biol Chem* 291:23618-23627.
538 10.1074/jbc.M116.741132

539

## Table 1(on next page)

AWC and AWA primary sensory neurons primary sensory neurons mediate the attraction to 17 odors.

Wild-type indicates N2 strain, AWC- indicates the ceh-36 mutant strain, AWA- indicates odr-7 mutant strain. Right column indicates the neuron(s) responsible for sensing each odor. Extra large dot = 0.6-1.0 attraction index (AI), large dot = 0.4-0.6 AI, medium dot = 0.2-0.4 AI, and small dot < 0.2 AI.

| odor | wild-type | AWC- | AWA- | AWA/AWC |
|---|---|---|---|---|
| diacetyl | ● | ● | • | AWA |
| benzaldehyde | ● | • | ● | AWC |
| butanone | ● | • | ● | AWC |
| isobutyric acid | ● | ● | • | AWA |
| 2-isobutyl thiazole | ● | • | ● | AWC |
| dimethylthiazole | ● | • | ● | AWC |
| 2,4,5-trimethylthiazole | ● | ● | ● | AWA or AWC |
| 2-methylpyrazine | ● | • | ● | AWC |
| 2-heptanone | ● | • | ● | AWC |
| 1-methylpyrrole | ● | • | ● | AWC |
| 4-chlorobenzyl mercaptan | ● | • | ● | AWC |
| butyric acid | ● | ● | • | AWA |
| 1-pentanol | ● | • | ● | AWC |
| benzyl mercaptan | ● | • | ● | AWC |
| 2-cyclohexylethanol | ● | • | ● | AWC |
| 2-ethoxythiazole | ● | • | ● | AWC |
| benzyl proprionate | ● | ● | • | AWA and AWC |

PeerJ Preprints | https://doi.org/10.7287/peerj.preprints.26451v1 | CC BY 4.0 Open Access | rec: 22 Jan 2018, publ: 22 Jan 2018

## Table 2 (on next page)

Timing of behavior change correlates with timing of GFP::EGL-4 nuclear accumulation.

Minutes to 50% animals with nuclear EGL-4 was calculated from the polynomial regression equation (see Methods) for each odor.

| odor | Minutes to 50% behavior change | Minutes to 50% animals with nuclear EGL-4 |
|---|---|---|
| 1-methylpyrrole | 80 | 76.6 |
| 2-ethoxythiazole | 90 | 59.2 |
| benzaldehyde | 90 | 69.7 |
| 4-chlorobenzyl mercaptan | 100 | 88.44 |
| 2,4,5-trimethylthiazole | 110 | 90.96 |

PeerJ Preprints | https://doi.org/10.7287/peerj.preprints.26451v1 | CC BY 4.0 Open Access | rec: 22 Jan 2018, publ: 22 Jan 2018

## Figure 1(on next page)

Real-time odor behavior assay.

(A) Assay design. Worms are placed in the middle of a 15 cm square plate. Odor solution is placed on one side of the plate, and a weak counterattractant (*E. coli* strain OP50) is placed on the opposite side. (B) Benzaldehyde attraction in real-time odor behavior assay. Attraction to the odor benzaldehyde (blue) decreases over the 2 hour assay. Control diluent (100% ethanol) attraction is shown in red.

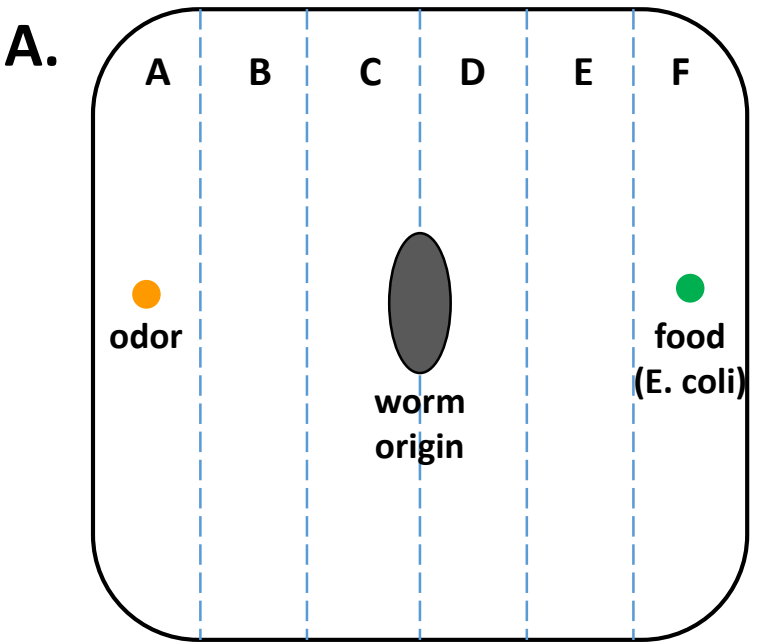


$$\text{Attraction index} = \frac{(2A + B) - (E + 2F)}{2(A+B+E+F)}$$

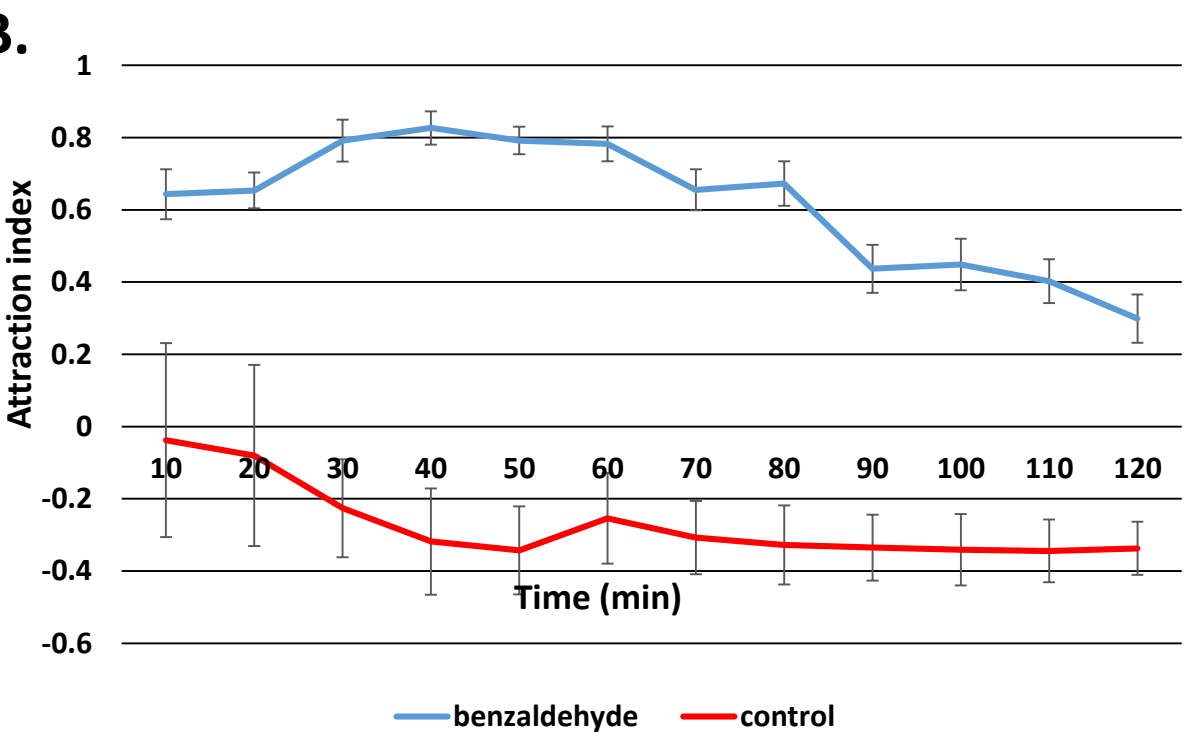


PeerJ Preprints | https://doi.org/10.7287/peerj.preprints.26451v1 | CC BY 4.0 Open Access | rec: 22 Jan 2018, publ: 22 Jan 2018

## Figure 2(on next page)

Short-term and long-term odor memory to the odor benzaldehyde in the real-time odor behavior assay.

Attraction over time with N2 wild type, *cng-3* short-term odor memory defective mutants, and *adp-1* short-term and long-term odor memory mutants in the standard behavior assay (A) and the real-time odor behavior assay (B). (C) Short-term odor memory in the standard and real-time behavior assays. Comparison of the 0’ and 40’ minute time points in (A) with the 30’ and 70’ minute time points in (B) for N2 and *cng-3* mutants. Error bars indicate standard error. Statistical significance calculated by student’s T-test. * indicates $p<0.05$, ** indicates $p<0.001$, NS indicates not significant.

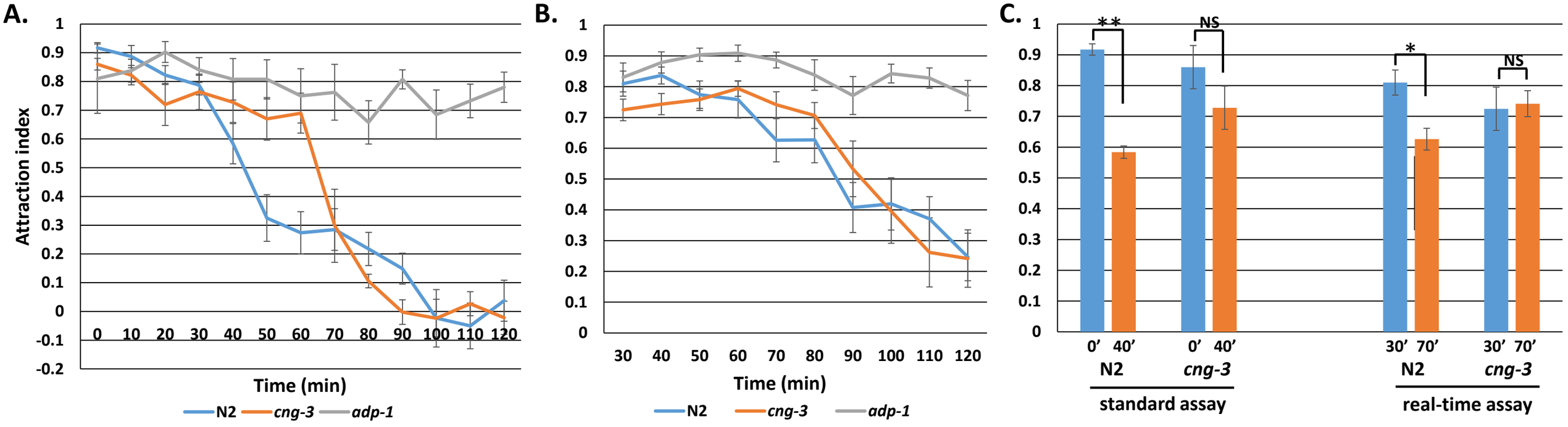


PeerJ Preprints | https://doi.org/10.7287/peerj.preprints.26451v1 | CC BY 4.0 Open Access | rec: 22 Jan 2018, publ: 22 Jan 2018

## Figure 3(on next page)

Temporal dynamics of odor memory for 12 different odors.

Purple dotted line marks approximate place where 50% of total behavior change occurs for each odor. Error bars indicate standard error.

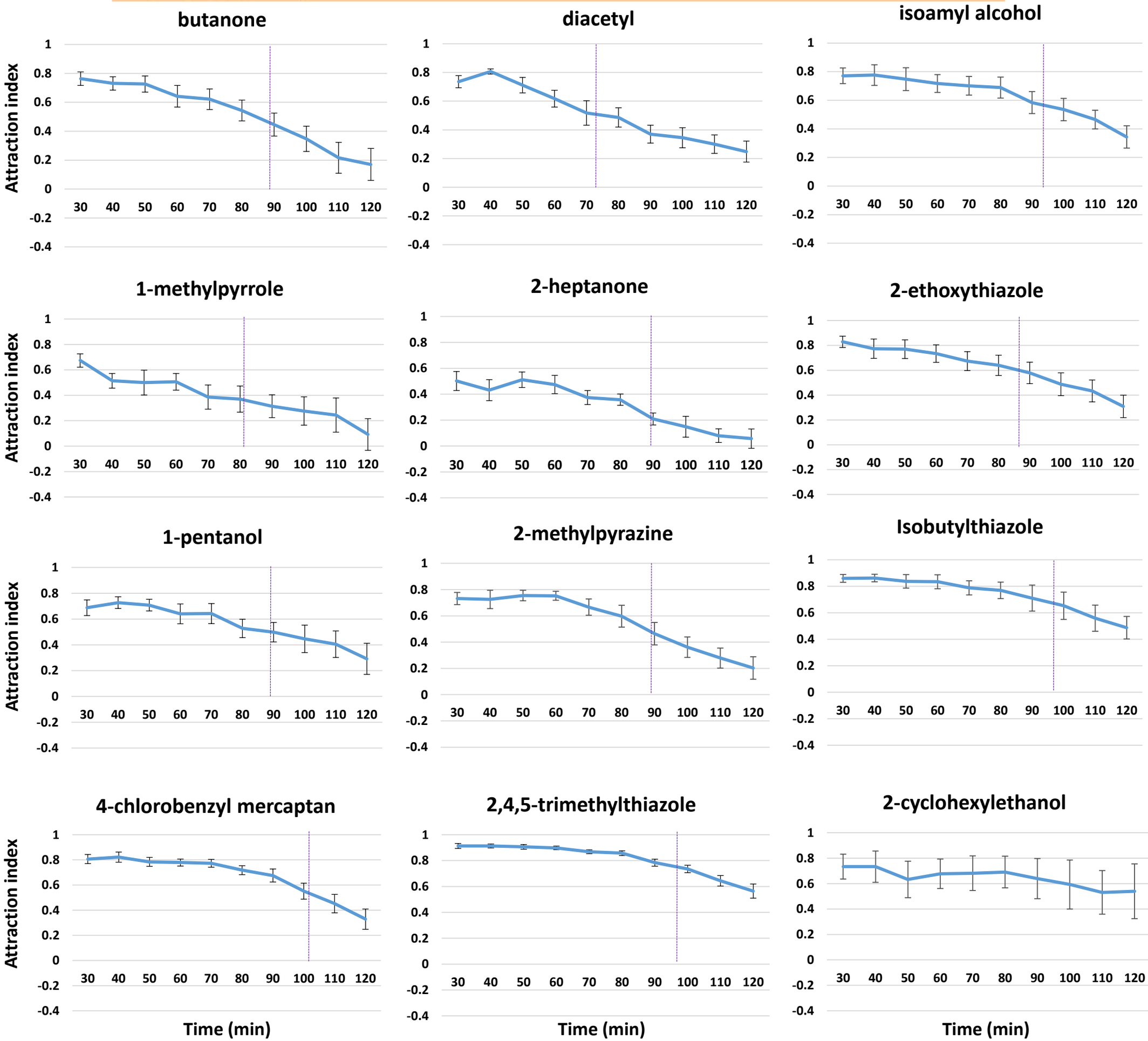


PeerJ Preprints | https://doi.org/10.7287/peerj.preprints.26451v1 | CC BY 4.0 Open Access | rec: 22 Jan 2018, publ: 22 Jan 2018

## Figure 4(on next page)

GFP::EGL-4 nuclear accumulation in early and late trending odors.

Animals were exposed to odor for indicated time and cytoplasmic/nuclear GFP::EGL-4 localization was observed. Early-trending odors are on the left, and late-trending odors on the right. A polynomial regression was calculated and regression curves are indicated on each graph. See Methods for individual regression equations. Error bars indicate standard error.

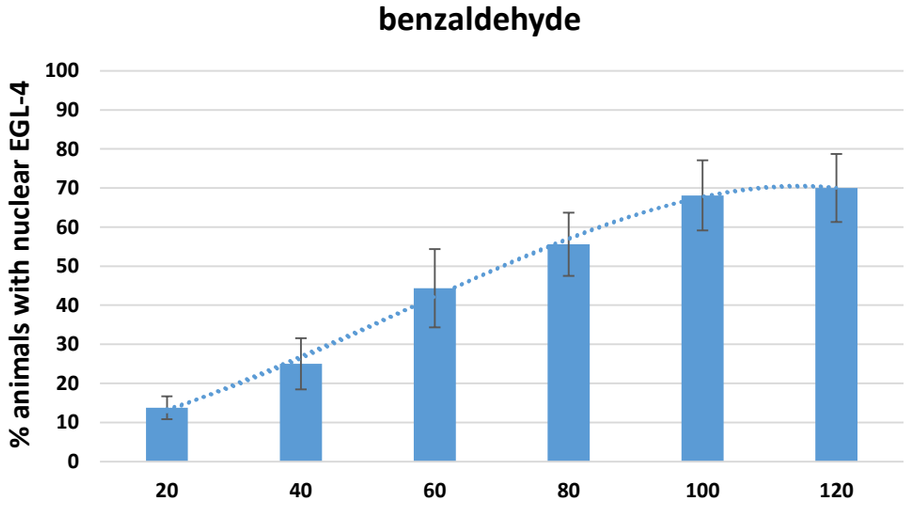


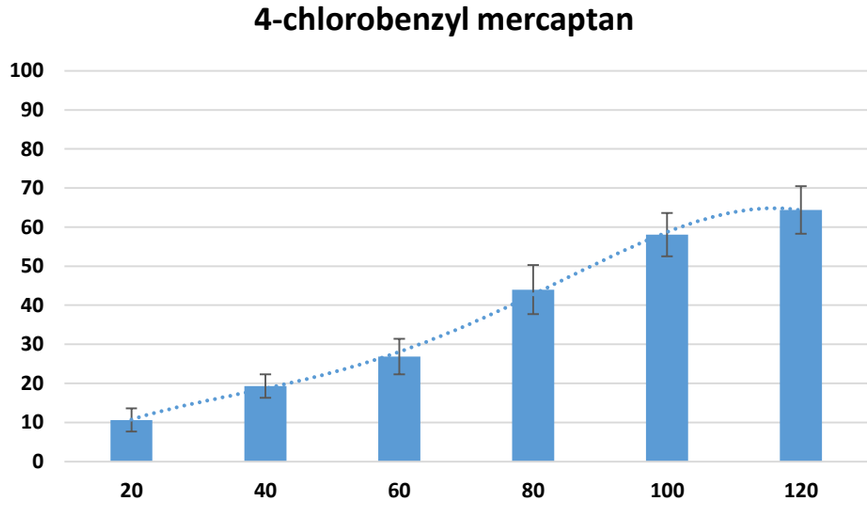


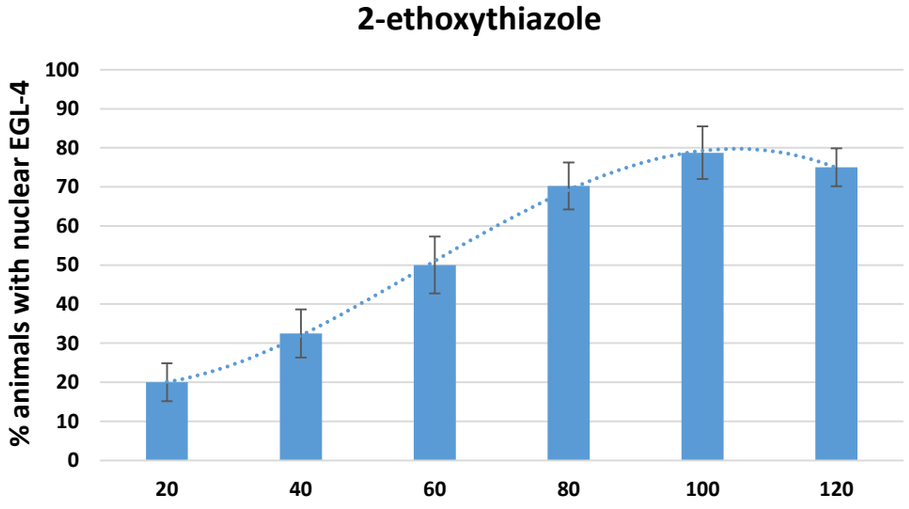


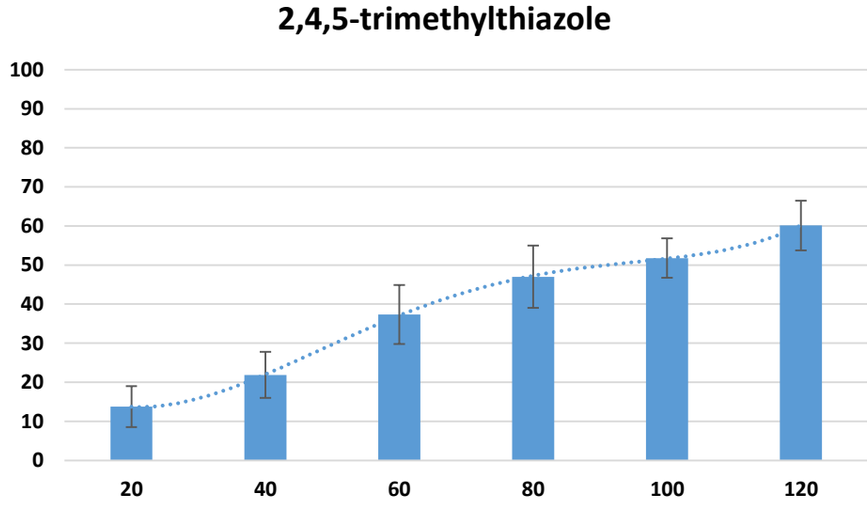


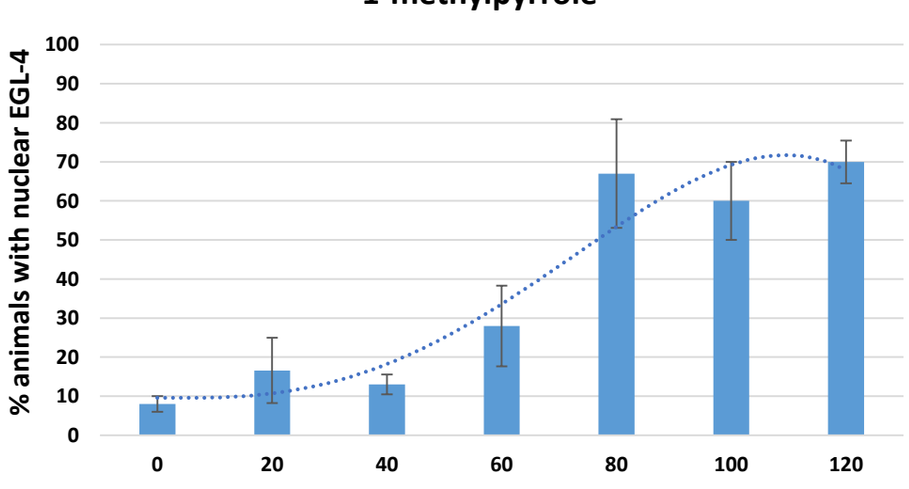


PeerJ Preprints | https://doi.org/10.7287/peerj.preprints.26451v1 | CC BY 4.0 Open Access | rec: 22 Jan 2018, publ: 22 Jan 2018